Substrate Binding in the FAD-Dependent Hydroxynitrile Lyase from Almond Provides Insight into the Mechanism of Cyanohydrin Formation and Explains the Absence of Dehydrogenation Activity[†,‡]

Ingrid Dreveny,[*,§] Aleksandra S. Andryushkova,[||] Anton Glieder,[||] Karl Gruber,[§] and Christoph Kratky[*,§]

Institut für Molekulare Biowissenschaften, Karl-Franzens-Universität, Humboldtstrasse 50/III, A-8010 Graz, Austria, and Institut für Molekulare Biotechnologie, Technische Universität Graz, Petersgasse 14/II, 8010 Graz, Austria

Received November 24, 2008; Revised Manuscript Received February 25, 2009

ABSTRACT: In a large number of plant species hydroxynitrile lyases catalyze the decomposition of cyanohydrins in order to generate hydrogen cyanide upon tissue damage. Hydrogen cyanide serves as a deterrent against herbivores and fungi. *In vitro* hydroxynitrile lyases are proficient biocatalysts for the stereospecific synthesis of cyanohydrins. Curiously, hydroxynitrile lyases from different species are completely unrelated in structure and substrate specificity despite catalyzing the same reaction. The hydroxynitrile lyase from almond shows close resemblance to flavoproteins of the glucose−methanol−choline oxidoreductase family. We report here 3D structural data of this lyase with the reaction product benzaldehyde bound within the active site, which allow unambiguous assignment of the location of substrate binding. Based on the binding geometry, a reaction mechanism is proposed that involves one of the two conserved active site histidine residues acting as a general base abstracting the proton from the cyanohydrin hydroxyl group. Site-directed mutagenesis shows that both active site histidines are required for the reaction to occur. There is no evidence that the flavin cofactor directly participates in the reaction. Comparison with other hydroxynitrile lyases reveals a large diversity of active site architectures, which, however, share the common features of a general active site base and a nearby patch with positive electrostatic potential. On the basis of the difference in substrate binding geometry between the FAD-dependent HNL from almond and the related oxidases, we can rationalize why the HNL does not act as an oxidase.

Hydroxynitrile lyases (HNLs)[1] are key enzymes in the process of cyanogenesis, which is widespread among higher plants, bacteria, fungi, and insects including major food crops like cassava, sorghum, and lima beans (*1*). Cyanogenic organisms release toxic hydrogen cyanide from damaged tissues as a defense agent against herbivoral and fungal attack (*2*). HNLs catalyze the last and crucial step in the reaction cascade, i.e., the decomposition of a cyanohydrin into HCN and the corresponding aldehyde or ketone. Several different classes of HNLs are known to date, some of which contain an FAD cofactor (FAD−HNL). Despite catalyzing the same reaction they differ in substrate specificity and do not share any significant homology on either sequence or structural level. Due to these substantial differences, HNLs from different species are believed to have evolved from unrelated precursor proteins by convergent evolution (*3, 4*). The importance of these enzymes as part of the "body armor" of an organism is also underlined by their generally high abundance in the tissues. In recent years HNLs have attracted considerable attention from industry, as the reverse reaction, the addition of HCN to a wide range of different aldehydes and ketones, can be exploited for the synthesis of enantiomerically pure cyanohydrins. The latter are important building blocks for the synthesis of several pharmaceutical and agrochemical products, such as anticoagulants and pyrethroid insecticides (*5*).

To date 3D structures are known for four HNLs. Three of them, the HNLs from *Hevea brasiliensis* (HbHNL *6, 7*), *Manihot esculenta* (MeHNL (*8*)), and *Sorghum bicolor* (SbHNL (*9*)), adopt α/β-hydrolase folds. The fourth, the FAD−HNL from *Prunus amygdalus* (almond, PaHNL), closely resembles glucose−methanol−choline (GMC) oxidoreductases despite not catalyzing a redox reaction (*10*). Members of this family include glucose oxidase (GOX), cholesterol oxidase (CHOX), pyranose 2-oxidase (POX), and aryl-alcohol oxidase (AAO) (*11*), but no other lyase. The role of the FAD cofactor in the reaction mechanism of PaHNL sparked much debate over the years (*12*−*15*). In the absence of a substrate, product, or inhibitor complex structure

[†] This work was supported by the Oesterreichischer Fonds zur Foerderung der wissenschaftlichen Forschung FWF through project P17132 and the DK Molecular Enzymology W901.

[‡] Structure factors and coordinates have been deposited in the Protein Data Bank as entries 3GDP (native structure) and 3GDN (complex with benzaldehyde).

* To whom correspondence should be addressed. C.K.: tel, +43 316 380 5417; fax, +43 316 380 9850; e-mail, Christoph.kratky@uni-graz.at. I.D.: Centre for Biomolecular Sciences, University of Nottingham, Nottingham NG7 2RD, U.K.; tel, +44 115 8268015; fax, +44 115 8468002; e-mail, ingrid.dreveny@nottingham.ac.uk.

[§] Karl-Franzens-Universität.

[||] Technische Universität Graz.

[1] Abbreviations: AAO, aryl-alcohol oxidase; CBDH, cellobiose dehydrogenase; CHOX, cholesterol oxidase; GMC, glucose−methanol−choline; Hb, *Hevea brasiliensis*; HNL, hydroxynitrile lyase; Me, *Manihot esculenta*; Pa, *Prunus amygdalus*; POX, pyranose 2-oxidase; Sb, *Sorghum bicolor*.

10.1021/bi802162s CCC: $40.75
Published on Web 03/03/2009

of an FAD−HNL, the reaction mechanism and the role of the FAD cofactor have been under discussion, with biochemical and modeling studies indicating an active site location near the flavin isoalloxazine ring (*12, 14, 16*−*18*). Based on these studies, a tentative catalytic mechanism was proposed involving general acid/base catalysis (*14*). However, the exact location and geometry of substrate binding are currently unknown.

We present here the crystal structure of the PaHNL1 isoform in complex with its natural reaction product benzaldehyde, resulting from a soaking experiment with the substrate mandelonitrile. The results unequivocally show for the first time the exact location of product/substrate binding within the active site and reveal the framework of interactions between reaction product and active site residues. A reaction mechanism is proposed that shares features with FAD-independent HNLs despite their differences in structure and sequence. A comparison with other GMC oxidoreductases leads us to conclude that the FAD cofactor is too far away from the substrate in order to directly participate in the reaction mechanism. Furthermore, the geometry of binding is not suited for oxidation of benzyl alcohol, the logical substrate in a potential oxidation reaction.

MATERIALS AND METHODS

Enzyme Purification and Crystallization. PaHNL was purchased from Sigma and purified, the isoforms were separated, and isoform 1 (PaHNL1) was crystallized as previously described (*10*). Crystallization drops (typical reservoir composition: 20% PEG 4000, 16% 2-propanol, and 0.1 M Na-Ada, pH 7.0) sometimes contained a monoclinic crystal form of space group $P2_1$, not readily distinguishable from the triclinic crystal form obtained in most of the crystallization experiments and used for the initial structure determination by multiple wavelength anomalous dispersion (*10*).

Data Collection, Processing, Model Building, and Refinement. Data sets of the monoclinic crystal form (unliganded and soaked with mandelonitrile) were collected at EMBL beamlines BW7B and X11 (DESY, Hamburg, Germany) equipped with a mar345 imaging plate detector at cryogenic temperatures. Prior to flash freezing, crystals where briefly soaked in a solution derived from the mother liquor by replacing half of the 2-propanol with 8% 2-methyl-2,4-pentanediol and adding 7% PEG 400 as additional cryoprotectant. Soaking conditions for incubation with the natural substrate were as follows: The crystals were transferred to 12 μL of the cryo solution. Then 1 μL of a racemic mixture of (*R*)- and (*S*)-mandelonitrile containing less than 3% contaminating benzaldehyde (kindly provided by DSM Fine Chemicals) was added with a syringe. After 2 min of soaking time the crystal was flash frozen in liquid nitrogen. The crystals belonged to space group $P2_1$ with cell parameters of $a = 69.1$ Å, $b = 93.7$ Å, $c = 87.3$ Å, and $\beta = 106.4°$. Data were processed with the DENZO and SCALEPACK program suite (*19*). Native Patterson maps and self-rotation functions were consistent with the presence of a noncrystallographic axis almost parallel to the crystallographic 2_1 screw axis resulting in a translational relation between the two molecules of the asymmetric unit. The structure was solved by molecular replacement using the structure from the triclinic PaHNL1 crystal form as the starting model. After one round of rigid body refinement, simulated annealing against a maximum-likelihood target to 2 Å resolution was carried out with the Crystallography and NMR System program suite (*20*). Several rounds of maximum-likelihood refinement and bulk solvent correction using all data over the whole resolution range were performed. Each cycle of refinement was followed by manual inspection of the electron density maps using the program O (*21*). During the whole refinement process no NCS restraints were applied in order to determine the differences between the two molecules. Water molecules were accepted based on the quality of the electron density. Only water molecules with *B*-factors less than 50 Å^2 and reasonable hydrogen-bonding geometry were retained. During the final refinement stages alternate conformations were modeled and refined. Some residual weak density in the $F_o - F_c$ maps results from the presence of further carbohydrate molecules at the glycosylation sites, which were impossible to model. The structure of liganded PaHNL1 was solved by rigid body refinement using the native $P2_1$ crystal structure. Clear additional electron density was visible in the $F_o - F_c$ maps. (*R*)-mandelonitrile and benzaldehyde were built with the program Sybyl (Tripos Inc., St. Louis, MO). In the active site the reaction product benzaldehyde was modeled into the density. A water molecule (at the expected position of the cyano group) was introduced by a peak search of the $F_o - F_c$ maps calculated with the benzaldehyde omitted. Due to the spherical shape of the density, water was chosen over cyanide as the predominant species present. Data collection and refinement statistics are summarized in Table 1. Figures were prepared with Molscript (*22*), Raster3D (*23*), and Pymol (DeLano Scientific, San Carlos, CA).

Table 1: Data Collection and Refinement Statistics

	native	liganded structure
space group	$P2_1$	$P2_1$
cell parameters		
a, *b*, *c* (Å)	69.1, 93.7, 87.3	69.0, 93.8, 86.9
α, *β*, *γ* (deg)	90.0, 106.4, 90.0	90.0, 106.5, 90.0
wavelength (Å)	0.8439	0.91010
D_{min} (Å)	1.57	1.67
completeness (%) (last shell)	96.7 (89.9)	87.7 (89.7)
total reflections	494321	502541
unique reflections	143518	107944
redundancy	3.4	4.7
$\langle I/\sigma I \rangle$ (last shell)	11.2 (2.6)	14.6 (7.4)
Wilson plot *B*-factor (Å^2)	11.6	16.1
R_{merge} (%) (last shell)	5.8 (38.5)	4.8 (16.0)
R-factor (%)	18.9	17.4
R-free (%)	20.5	19.8
no. of residues (atoms)	1042 (7988)	1042 (7938)
FADs (atoms)	2 (106)	2 (106)
ligands (atoms)	2 (8)	6 (56)
carbohydrates (atoms)	21 (264)	17 (215)
waters	1589	1269
⟨*B*-factors⟩ (Å^2)		
main chain atoms	10.4	13.7
side chain atoms	12.3	15.5
waters	26.3	27.7
FAD	5.6	8.6
carbohydrates	33.5	35.3
ligand in active site		22.7
other ligands	18.7	28.8
Ramachandran plot (%)		
core region	91.4	89.3
additionally allowed	8.4	10.5
generously allowed	0.2	0.2

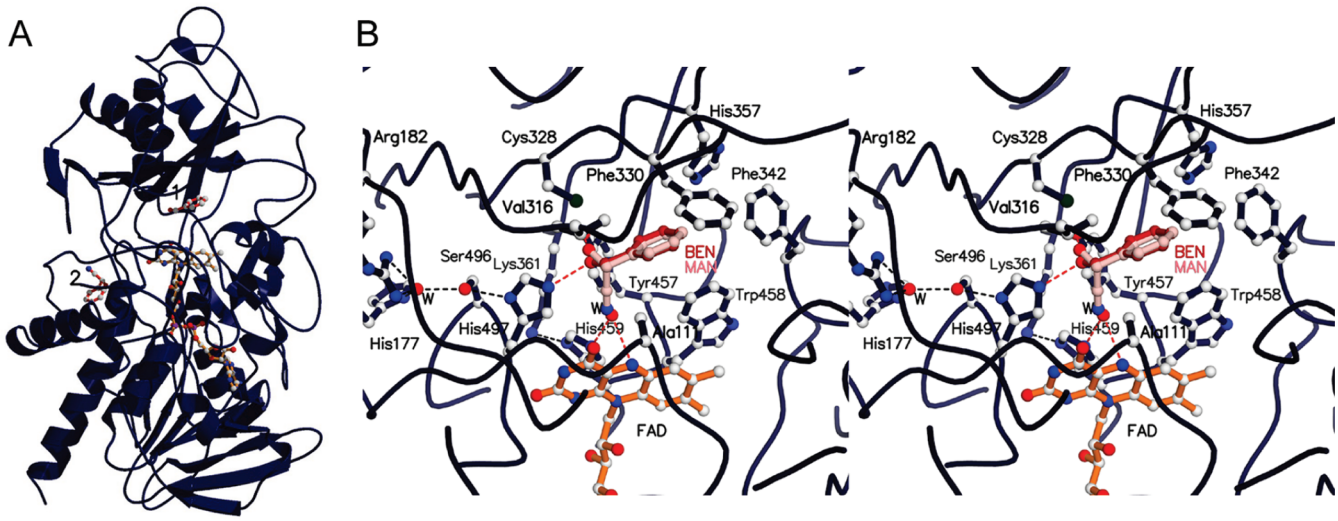

FIGURE 1: (A) Ligand binding sites in PaHNL1. Ribbon diagram of PaHNL1 (blue) with the flavin cofactor depicted in orange ball-and-stick representation indicating the substrate binding sites. Ligands are highlighted in red ball-and-stick representation, and the binding sites are numbered as 1 for the active site and 2 for the hydrophobic pocket. For clarity, carbohydrates at the glycosylation sites have been omitted in the figure. (B) Stereo representation of the active site region. The binding mode of the reaction product benzaldehyde with the active site water (red) and the modeled (*R*)-mandelonitrile (pink) are shown. Plausible hydrogen-bonding interactions are indicated by red dashed lines. The hydrogen-bonding network surrounding the active site residues His459 and His497 is indicated by black dashed lines.

PaHNL1 Mutagenesis, Expression, and Enzymatic Assay. Site-directed mutagenesis of PaHNL1 to introduce His459Asn and His497Asn mutations was carried out using the Stratagene QuickChange XL kit. Both mutants were expressed in *Pichia pastoris* X33 with pGAPZA-PaHNL1 as positive control and *P. pastoris* X-33 as negative control in 200 mL of BMD 1% media (100 mM potassium phosphate, pH 6.0, 1.34% YNB, 4×10^{-5}% biotin, 1% glucose) for 3 days at 28 °C. Cultures were harvested and the supernatant media concentrated to approximately 1 mL. Expression levels of secreted proteins were assessed by SDS−PAGE. Activity measurements were carried out in parallel for the mutants, wild-type PaHNL1, and the negative control by using mandelonitrile as substrate and following the increase in absorption at 280 nm (*24*). Due to the background of the concomitant chemical reaction, the low activities of the mutants were not exactly quantifiable.

RESULTS

Overall Structure and Binding Sites. PaHNL1 crystals of space group $P2_1$ grew under similar conditions as the triclinic crystals used previously to solve the original structure (*10*). Monoclinic crystals were used to collect a native data set (to 1.57 Å resolution) and for soaking with the substrate mandelonitrile (data set to 1.67 Å resolution). The unliganded structure was found to agree with the model derived from the triclinic data (maximum rmsd of Cα atoms: 0.54 Å, loop region 222−225 excluded). Interestingly, difference density appeared at two sites after soaking with mandelonitrile. The locations of these binding sites are shown in Figure 1A. One of them is within the putative active site, i.e., at the interface of the two protein domains above the residue of the flavin isoalloxazine ring (Figure 2B). Close inspection of this density indicated that it originates from the reaction product (benzaldehyde) rather than the substrate (mandelonitrile), although the presence of a fraction of uncleaved substrate at low occupancy cannot be excluded. Observation of a product molecule in the active site is not surprising, since the soaking experiment was conducted with a crystal of active native enzyme. A molecule of benzaldehyde and a water molecule were fitted into this density. Comparison of the benzaldehyde *B*-factors with the *B*-factors of surrounding residues indicates binding of the ligand with high occupancy.

The active site region with its hydrogen-bonding interactions is shown in Figure 1B; hydrogen bonds exist between benzaldehyde and the hydroxyl group of Tyr457 and the imidazole ring of His497 as well as between the active site water (presumably located in a similar position as the reaction cyanide) and the His459 imidazole and N5 of the flavin. His459 is in hydrogen-bonding interaction with Lys361, whereas His497 is hydrogen bonded to Ser496, which in turn is interacting with a water molecule that interacts with His177 and Arg182. The benzaldehyde aromatic ring is embedded in a hydrophobic pocket consisting of residues Ala111, Val316, Cys328, Phe330, Phe342, His357, and Trp458. Comparison with the unliganded structure (Figure 2A,B) reveals that two of the three active site water molecules are displaced by benzaldehyde, whose binding otherwise induces only minor structural rearrangements of amino acid side chains (Phe330, Ser332, Phe342, and Trp458).

In view of the known *R*-selectivity, modeling of the natural substrate (*R*)-mandelonitrile into the active site is straightforward. In order to obtain the correct enantiomer, the cyano group of the substrate (as well as the site of the cyanide ion in the reverse reaction) must point toward the active site water molecule sequestered between benzaldehyde and the cofactor (Figure 2B). This results in a binding geometry which agrees well with results from previous docking studies (*14*). The cyanohydrin hydroxyl group is held in place by interactions with Cys328, Tyr457, and His497, while the cyano group is pointing toward His459 and N5 of the FAD isoalloxazine ring, displacing the active site water (Figure 1B).

In the complex structure, clear density for (*R*)-mandelonitrile can be seen in a hydrophobic pocket at a second location, which is occupied by a molecule of 2-propanol in the

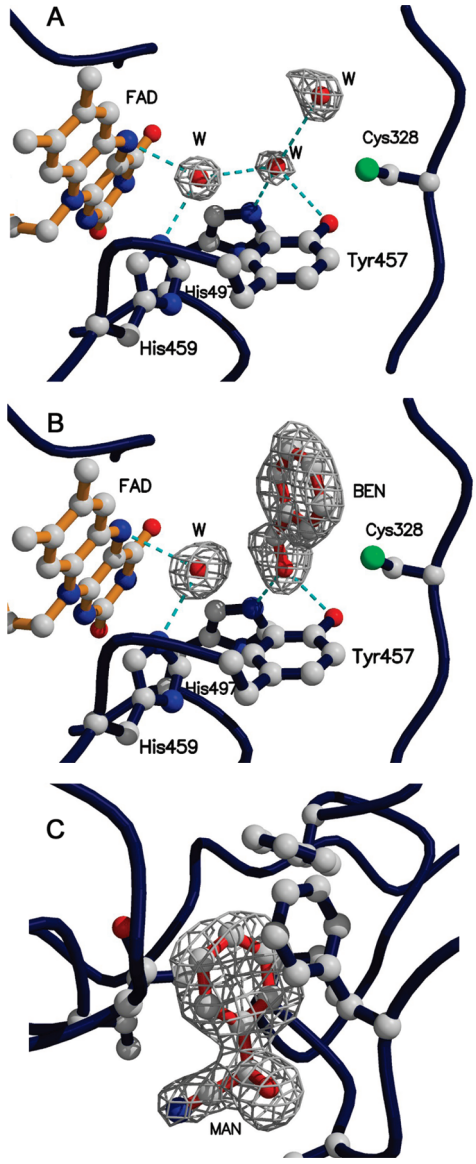

FIGURE 2: (A) Water molecules within the active site of the native structure. Ribbon representation of the PaHNL1 active site region (blue) with important residues in ball-and-stick representation. $F_o - F_c$ electron densities (gray) of active site water molecules in the native monoclinic crystal form. Plausible hydrogen-bonding interactions are indicated by dashed lines in cyan. (B) Benzaldehyde within the active site in the liganded structure. $F_o - F_c$ density in the active site of the liganded structure (gray). Benzaldehyde and the active site water are depicted in red. The orientation of the active site region is shown as in the native structure. (C) Mandelonitrile binding site in a hydrophobic pocket. The $F_o - F_c$ electron density of uncleaved mandelonitrile (in red ball-and-stick representation) in the hydrophobic pocket of the liganded structure is shown, indicating that this site has no catalytic function.

unliganded PaHNL1 structure (*10*). Apparently, the site discriminates against (*S*)-mandelonitrile, as racemic mandelonitrile was used for the soaking experiments. The density corresponds to an uncleaved substrate molecule, indicating that no catalytic activity can be attributed to this location (Figure 2C). This hydrophobic pocket is not conserved in the related GMC oxidoreductases.

Site-Directed Mutagenesis. FAD−HNLs are highly homologous and typically share over 60% sequence identity. With a few exceptions (see below), all of the active site residues are conserved. In order to delineate the role of the two active site histidines, we mutated His497 and His459 to asparagine and expressed both mutants and wild-type PaHNL1 as secreted proteins in *P. pastoris*. Activity measurements with the substrate mandelonitrile revealed that both mutants showed less than 5% activity compared to wild type, indicating that both residues are essential for the cleavage reaction.

Superposition with Other GMC Oxidoreductase Ligand Complexes. Available structural data of GMC oxidoreductases in complex with substrates, products, or inhibitors include cholesterol oxidase (CHOX) with the steroid substrate dehydroisoandrosterone (*25*), cellobiose dehydrogenase (CBDH) in complex with the inhibitor cellobiono-1,5-lactam (*26*), and pyranose 2-oxidase (POX) in complex with the reaction product 2-keto-β-D-glucose (*27*), the slow substrate 2-fluoro-2-deoxy-D-glucose (*28*), or the weak inhibitor acetate (*29*). Superposition of these structures based on the pteridin moiety of flavin with the PaHNL1−benzaldehyde structure and mandelonitrile-bound model are shown in Figure 3. The structures superimpose well (at least 70% of residues within 3 Å rmsd cutoff), including the conformation of active site residues.

Strikingly, the complex structures of all known GMC oxidoreductases overlap in a single point close to the flavin N5 atom at about 3.2 Å distance and an angle with the flavin N10−N5 atoms of ~102° (Figure 3). In POX and CBDH, carbon atoms C2 and C1 of the ligands (site of oxidative attack in the proposed binding mode of the natural substrates) are located at this position (*26, 27*). In CHOX it is an active site water (*25*). For GOX, modeling studies place β-D-glucose in close proximity to the flavin (*30*), displacing the active site water molecule, similar to the POX−product complex (*27*).

An active site histidine is the only residue that is strictly conserved throughout the GMC oxidoreductase family (His459 in PaHNL1, His447 in CHOX, His516 in *Aspergillus niger* GOX, His689 in CBDH, and His548 in POX). This histidine was implicated in proton abstraction from the substrate in POX (*27*), CBDH (*26*), and GOX (*31, 32*), while it is hydrogen bonded to the active site water in the substrate complex structure of CHOX (*25*). Strikingly, in PaHNL1 it is the cyano group that points toward the strictly conserved His459 and not the cyanohydrin's hydroxyl group. The other well-conserved active site residue is an asparagine in POX, CHOX, and CBDH, which is replaced by a second histidine in AAO, GOX, and PaHNL1 (His497). Mutation of this residue also has severe consequences for enzyme activity in all GMC oxidoreductases examined (*33*−*36*). Substrates are consistently about equidistantly bound between these two important active site residues in POX, CBDH, and the GOX and the AAO model), whereby the hydroxyl group, site of oxidative attack, forms hydrogen-bonding interactions to both side chains. In PaHNL1, however, the hydroxyl group of (*R*)-mandelonitrile is held in place by interactions with His497, Tyr457, and Cys328 and is not sandwiched between His459 and His497.

DISCUSSION

Reaction Mechanism of PaHNL. The reversible cleavage of α-cyanohydrins into HCN and the corresponding aldehyde or ketone follows an ordered Uni Bi mechanism whereby the aldehyde is the first substrate to be bound in the

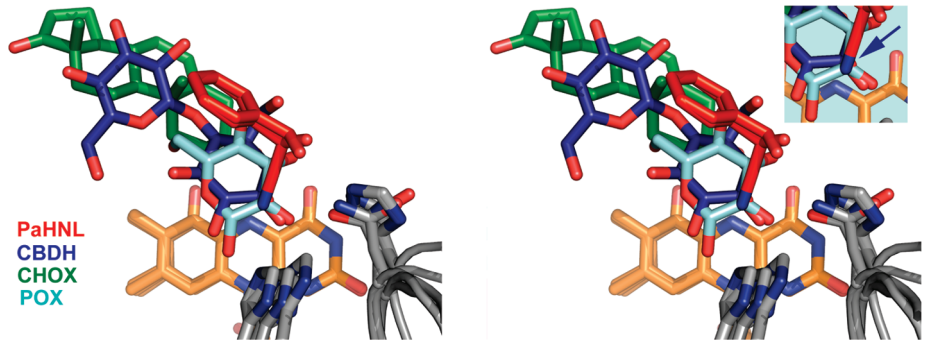

FIGURE 3: Stereo representation of the superposition of GMC oxidoreductase structures in complex with the respective substrate, inhibitor, or product with the PaHNL1 benzaldehyde complex structure and modeled (*R*)-mandelonitrile. Structures of CHOX with the steroid substrate dehydroisoandrosterone (*25*) (ligand shown in green), CBDH in complex with the inhibitor cellobiono-1,5-lactam (*26*) (ligand shown in dark blue), and POX in complex with the reaction product 2-keto-β-D-glucose (*27*) (ligand shown in light blue) are superimposed with PaHNL1−benzaldehyde and modeled (*R*)-mandelonitrile (ligands both shown in red). Superimposed FAD cofactors are depicted in orange, and the two important catalytic residues (His459 and His497 in PaHNL) are shown in light gray. Note the culmination of these structures in a single point close to the flavin isoalloxazine ring N5 atom (drawn in a close-up and highlighted by an arrow) and the mostly conserved active site residues.

Scheme 1: Proposed Mechanism of the PaHNL1 Cyanohydrin Cleavage Reaction[a]

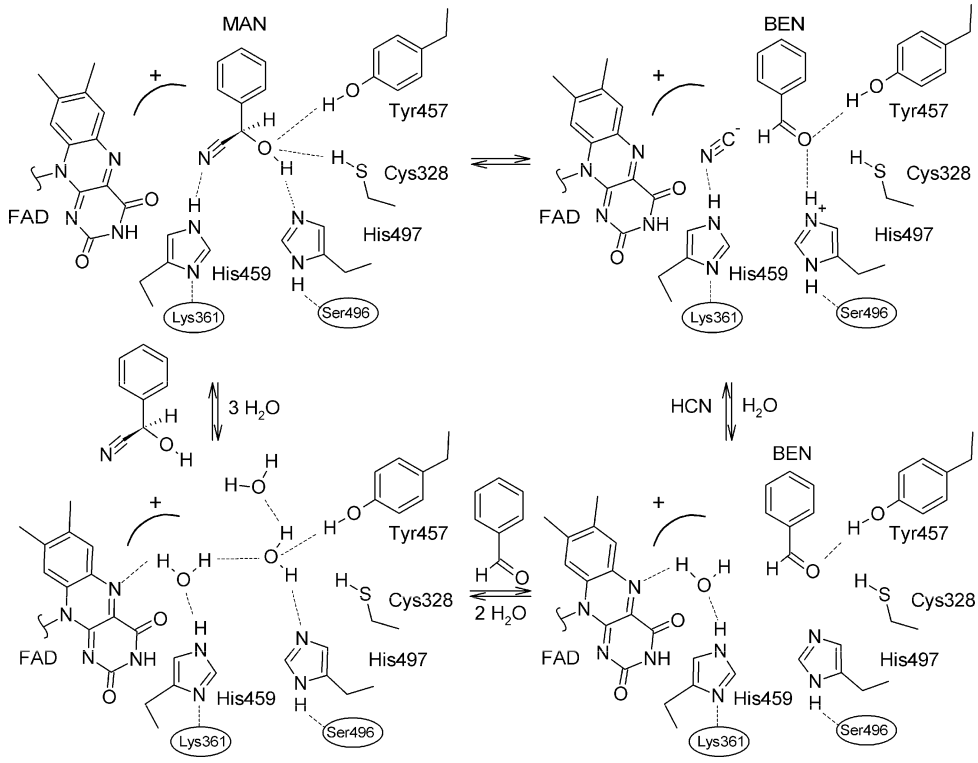

[a] The reaction proceeds via general acid/base catalysis through residue His497. The cyanide is stabilized by the overall positive electrostatic potential in the active site region (indicated by a positive charge). The mechanistic details of the reprotonation of cyanide are currently unresolved, but it is likely that His459 is involved in this step. Plausible hydrogen-bonding interactions are indicated by dashed lines. Active site residues are labeled. According to the ordered Uni Bi mechanism benzaldehyde is the last product to leave the active site.

condensation reaction (*13*). Together with the structural, mutational, and available biochemical evidence, we propose the mechanism for the reversible cyanohydrin cleavage reaction depicted in Scheme 1: while the (*R*)-mandelonitrile phenyl group is held in place by numerous hydrophobic interactions, His497 is proposed to act as a general base abstracting the proton from the mandelonitrile hydroxyl group; the modeled complex with mandelonitrile shows that its hydroxyl group is within hydrogen-bonding distance to His497, Cys328, and Tyr457. Cys328 can be ruled out as a general base as it is not conserved among all FAD−HNLs (isoleucine or valine is also observed at this position). The pK_a values of the corresponding free amino acids argue for His497 rather than Tyr457 as the general base (the pH optimum of the enzyme is about 5.5). In fact, the interaction network around the mandelonitrile-OH suggests that His497-Nε2 is unprotonated, since Cys328 and Tyr457 both have to act as hydrogen bond donors to the mandelonitrile-OH for lack of any other hydrogen-bonding partner in their vicinity. The only consistent H-bonding network thus assigns His497 the role of H-bond acceptor. While previous biochemical studies had implicated the involvement of a cysteine residue (*37*), the observation that covalent modification of this cysteine abolishes catalytic activity is readily explained

by the close proximity between Cys328 and the substrate binding site.

His459, the second active site histidine, is probably responsible for protonation of the cleaved cyanide ion. Protonation of cyanide should be facilitated by an increase in the acidity of His459 (Nε2 of its imidazole ring is 2.9 Å away from the cyano group) due to its interaction with Lys361 (Figure 1B). Interestingly, the hydroxyl group of mandelonitrile points away from the flavin N5 atom, suggesting that N5 is not directly involved in the reaction mechanism. This is in line with our previous assertion that the flavin does not directly participate in the reaction mechanism (at least not in a redox role), that an oxidized cofactor is solely required for electrostatic reasons (*14*), and that substitution at the N5 atom interferes with substrate turnover for steric reasons. We conclude that FAD is an evolutionary remnant from an oxidoreductase precursor whose presence is necessary for the structural integrity of FAD−HNLs. A positive potential at the active site was originally inferred from inhibition studies with a variety of different alcohols, carboxylic acids, and inorganic anions (*16*). The structure shows that this positive potential, facilitating cyanide ion formation (*10, 14*), is mainly provided by residues Arg194, Arg300, Lys361, and Arg182.

A Common Mechanism for All Hydroxynitrile Lyases? In solution, cyanohydrin cleavage occurs spontaneously at high pH and is initiated by the deprotonation of the cyanohydrin's hydroxyl group.

Based on these observations, Becker and Pfeil postulated many years ago that the active site of a hydroxynitrile lyase should at least encompass a suitably positioned general base to abstract a proton from the cyanohydrin hydroxyl group and a nearby positive potential to stabilize the emerging cyanide ion (*38*). It is an intriguing question if and how these requirements are fulfilled in the variety of different HNLs. The first hydroxynitrile lyase whose reaction mechanism was elucidated on the basis of comprehensive structural, kinetic, and mutagenesis data is the one from *H. brasiliensis*, which exhibits a stereospecificity opposite to FAD−HNLs (*39*−*41*). In this enzyme, the catalytic triad (Ser80-His236-Asp207) undoubtedly acts as general base for the deprotonation of the cyanohydrin hydroxyl group, and an active site lysine (Lys236) provides the positive charge to stabilize the cyanide (*40, 42*). A similar mechanism was proposed for the related enzyme MeHNL (*8, 43*). SbHNL also adopts an α/β hydrolase fold but is related to carboxypeptidases. While its catalytic triad serine is too far away to deprotonate the substrate (*9*), the carboxylate group of the C-terminal residue (Trp270) was proposed to act as the general base, assisted by an active site water molecule (*9*). Stabilization of the cyanide by a positive electrostatic potential within the active site has not yet been confirmed for this enzyme.

PaHNL conforms to the requirements postulated for HNL catalysis, although in a very unique fashion. Deprotonation of the substrate and reprotonation of the cleaved cyanide is accomplished by two histidines "inherited" from its precursor oxidoreductase and adapted to the specific requirements of HNL catalysis. Unlike in HbHNL, where a positive electrostatic potential is produced by a single lysine residue, PaHNL has several positively charged residues surrounding the active site to stabilize the nascent cyanide. It will be fascinating to see how convergent evolution has implemented the requirements of HNL catalysis into enzymes belonging to yet other fold families, such as the hydroxynitrile lyase from flax, which belongs to the family of Zn-dependent alcohol dehydrogenases (*44*).

Features of Substrate Binding in GMC Oxidoreductases. In flavoenzymes the sites of oxidative attack typically cluster in a well-defined position "in front" of the N5 of the FAD isoalloxazine ring at approximately 3.5−3.8 Å distance and at an angle N10(FAD)−N5(FAD)−CH(substrate) in a narrow range of 96−117° (*45*). As shown in Figure 3 this is also true for the GMC oxidoreductases POX, CBDH, and most likely GOX and AAO based on substrate−enzyme modeling studies (*26, 27, 30, 31, 34, 36*). An exception is the CHOX−substrate crystal structure, where the angle N10−N5−CH is much larger (162°) (*25*). However, CHOX catalyzes an oxidation and isomerization step, and the crystal structure is unlikely to represent the actual Michaelis complex as soaking was performed under reducing conditions. It is likely that the active site water in the structure, which is sandwiched between the conserved histidine and the asparagine, mimics the substrate's hydroxyl group (*46*).

A hydride transfer mechanism has generally been proposed for GMC oxidoreductases although a radical mechanism cannot completely be ruled out at present (*26, 32, 46, 47*). The well-defined position of the site of oxidative attack is thought to be required for optimal orbital overlap in an efficient hydride transfer to the flavin N5 atom (*45*). A potential two-step radical mechanism would require similar distance restraints. The only strictly conserved residue within GMC oxidoreductases, the active site histidine (His459 in PaHNL1), is well positioned to deprotonate the substrate. The main difference between the oxidoreductases and PaHNL1 lies in the orientation of the substrates' hydroxyl groups, which points toward the flavin N5 and the conserved histidine in the oxidoreductases, but away from N5 in PaHNL1, where it is the nitrogen atom of the cyano group that occupies the strategic position close to N5. Consequently, the cyanohydrin hydroxyl group is not within reach of the conserved His459 (over 5 Å away), and it is the second active site histidine, His497, that acts as general base.

FAD−HNLs as Oxidases? Benzaldehyde is not further oxidized by PaHNL (*12, 13*), nor has any other oxidation substrate been reported, yet PaHNL shows all of the main features of an oxidase (*12, 13, 48, 49*). The redox potential of the cofactor should be sufficiently high based on its positive electrostatic potential environment (even more positive than in the related oxidases), which should stabilize the anionic reduced form of the cofactor. We previously speculated that FAD−HNLs may have evolved from an aryl-alcohol oxidase precursor protein, given that GMC oxidoreductases generally oxidize nonactivated alcohols and in view of the similarity to aryl-alcohol oxidase sequences (*10*). Consequently, a potential substrate would be benzyl alcohol, which can safely be assumed to occupy the same position as benzaldehyde. Benzyl alcohol is known to act as competitive inhibitor of FAD−HNLs in the reversible cyanohydrin cleavage reaction (*16, 50*). From the complex structure it is now evident that the site of hypothetical oxidative attack on benzyl alcohol is located ∼5.6 Å away from the flavin N5, clearly too far away for a direct hydride transfer. Therefore, it is highly unlikely that PaHNL acts as an oxidase on this substrate. In addition, His459, which is strictly conserved

among the oxidases, probably carries a hydrogen atom at Nε2, which would make it a very unlikely general base for any other potential substrate with a binding geometry more similar to the oxidases. Taken together, we conclude that PaHNL1 is not suitable for oxidizing benzyl alcohol based on the predicted binding geometry. We anticipate that an alcohol substrate that points a hydroxyl group toward the N5 similar to other oxidases is also unlikely to be oxidized by PaHNL1.

ACKNOWLEDGMENT

We thank Ulrike Wagner, Helmut Schwab, and Herfried Griengl for interesting discussions and the support of this work and acknowledge the beamline scientists at EMBL—Hamburg for their help. We acknowledge Jonas Emsley for critically reading the manuscript.

REFERENCES

1. Conn, E. E. (1981) in *The Biochemistry of Plants: A Comprehensive Treatise* (Stumpf, P. K., and Conn, E. E., Eds.) pp 479−500, Academic Press, New York.
2. Nahrstedt, A. (1985) Cyanogenic compounds as protecting agents for organisms. *Plant Syst. Evol. 150*, 35–47.
3. Hickel, A., Hasslacher, M., and Griengl, H. (1996) Hydroxynitrile lyases: functions and properties. *Physiol. Plant. 98*, 891–898.
4. Wajant, H., and Effenberger, F. (1996) Hydroxynitrile lyases of higher plants. *Biol. Chem. 377*, 611–617.
5. Purkarthofer, T., Skranc, W., Schuster, C., and Griengl, H. (2007) Potential and capabilities of hydroxynitrile lyases as biocatalysts in the chemical industry. *Appl. Microbiol. Biotechnol. 76*, 309–320.
6. Gruber, K., Gugganig, M., Wagner, U. G., and Kratky, C. (1999) Atomic resolution structure of hydroxynitrile lyase from *Hevea brasiliensis*. *Biol. Chem. 380*, 993–1000.
7. Wagner, U. G., Hasslacher, M., Griengl, H., Schwab, H., and Kratky, C. (1996) Mechanism of cyanogenesis: the crystal structure of hydroxynitrile lyase from *Hevea brasiliensis*. *Structure 4*, 811–822.
8. Lauble, H., Förster, S., Miehlich, B., Wajant, H., and Effenberger, F. (2001) Structure of hydroxynitrile lyase from *Manihot esculenta* in complex with substrates acetone and chloroacetone: implications for the mechanism of cyanogenesis. *Acta Crystallogr. D57*, 194–200.
9. Lauble, H., Miehlich, B., Forster, S., Wajant, H., and Effenberger, F. (2002) Crystal structure of hydroxynitrile lyase from *Sorghum bicolor* in complex with the inhibitor benzoic acid: a novel cyanogenic enzyme. *Biochemistry 41*, 12043–12050.
10. Dreveny, I., Gruber, K., Glieder, A., Thompson, A., and Kratky, C. (2001) The hydroxynitrile lyase from almond: a lyase that looks like an oxidoreductase. *Structure 9*, 803–815.
11. Cavener, D. R. (1992) GMC oxidoreductases. A newly defined family of homologous proteins with diverse catalytic activities. *J. Mol. Biol. 223*, 811–814.
12. Bärwald, K. R., and Jaenicke, L. (1978) D-hydroxynitrile lyase: involvement of the prosthetic flavin adenine dinucleotide in enzyme activity. *FEBS Lett. 90*, 255–260.
13. Jorns, M. S. (1979) Mechanism of catalysis by the flavoenzyme oxynitrilase. *J. Biol. Chem. 254*, 12145–12152.
14. Dreveny, I., Kratky, C., and Gruber, K. (2002) The active site of hydroxynitrile lyase from *Prunus amygdalus*: modeling studies provide new insights into the mechanism of cyanogenesis. *Protein Sci. 11*, 292–300.
15. Bornemann, S. (2002) Flavoenzymes that catalyse reactions with no net redox change. *Nat. Prod. Rep. 19*, 761–772.
16. Jorns, M. S. (1980) Studies on the kinetics of cyanohydrin synthesis and cleavage by the flavoenzyme oxynitrilase. *Biochim. Biophys. Acta 613*, 203–209.
17. Glieder, A., Weis, R., Skranc, W., Poechlauer, P., Dreveny, I., Majer, S., Wubbolts, M., Schwab, H., and Gruber, K. (2003) Comprehensive step-by-step engineering of an (R)-hydroxynitrile lyase for large-scale asymmetric synthesis. *Angew. Chem., Int. Ed. Engl. 42*, 4815–4818.
18. Weis, R., Gaisberger, R., Skranc, W., Gruber, K., and Glieder, A. (2005) Carving the active site of almond R-HNL for increased enantioselectivity. *Angew. Chem., Int. Ed. Engl. 44*, 4700–4704.
19. Otwinowski, Z., and Minor, W. (1997) Processing of X-ray diffraction data collected in oscillation mode. *Methods Enzymol. 276*, 307–326.
20. Brünger, A. T., Adams, P. D., Clore, G. M., Delano, W. L., Gros, P., Grosse-Kunstleve, R. W., Jiang, J. S., and Warren, G. L. (1998) Crystallography and NMR system (CNS): a software system for macromolecular structure determination. *Acta Crystallogr. D54*, 905–921.
21. Jones, T. A., Zou, J. Y., Cowan, S., and Kjeldgaard, M. (1991) Improved methods for building protein models in electron density maps and the location of errors in these models. *Acta Crystallogr. A47*, 110–119.
22. Kraulis, P. J. (1991) MOLSCRIPT: a program to produce both detailed and schematic plots of protein structures. *J. Appl. Crystallogr. 24*, 946–950.
23. Merritt, E. A., and Bacon, D. J. (1997) Raster3D: photorealistic molecular graphics. *Methods Enzymol. 277*, 505–524.
24. Weis, R., Poechlauer, P., Bona, R., Skranc, W., Luiten, R., Wubbolts, M., Schwab, H., and Glieder, A. (2004) Biocatalytic conversion of unnatural substrates by recombinant almond R-HNL isoenzyme 5. *J. Mol. Catal. B: Enzym. 29*, 211–218.
25. Li, J., Vrielink, A., Brick, P., and Blow, D. M. (1993) Crystal structure of cholesterol oxidase complexed with a steroid substrate: implications for flavin adenine dinucleotide dependent alcohol oxidases. *Biochemistry 32*, 11507–11515.
26. Hallberg, B. M., Henriksson, G., Pettersson, G., Vasella, A., and Divne, C. (2003) Mechanism of the reductive half-reaction in cellobiose dehydrogenase. *J. Biol. Chem. 278*, 7160–7166.
27. Bannwarth, M., Heckmann-Pohl, D., Bastian, S., Giffhorn, F., and Schulz, G. E. (2006) Reaction geometry and thermostable variant of pyranose 2-oxidase from the white-rot fungus *Peniophora* sp. *Biochemistry 45*, 6587–6595.
28. Kujawa, M., Ebner, H., Leitner, C., Hallberg, B. M., Prongjit, M., Sucharitakul, J., Ludwig, R., Rudsander, U., Peterbauer, C., Chaiyen, P., Haltrich, D., and Divne, C. (2006) Structural basis for substrate binding and regioselective oxidation of monosaccharides at C3 by pyranose 2-oxidase. *J. Biol. Chem. 281*, 35104–35115.
29. Hallberg, B. M., Leitner, C., Haltrich, D., and Divne, C. (2004) Crystal structure of the 270 kDa homotetrameric lignin-degrading enzyme pyranose 2-oxidase. *J. Mol. Biol. 341*, 781–796.
30. Meyer, M., Wohlfahrt, G., Knablein, J., and Schomburg, D. (1998) Aspects of the mechanism of catalysis of glucose oxidase: a docking, molecular mechanics and quantum chemical study. *J. Comput.-Aided Mol. Des. 12*, 425–440.
31. Wohlfahrt, G., Witt, S., Hendle, J., Schomburg, D., Kalisz, H. M., and Hecht, H. J. (1999) 1.8 and 1.9 Å resolution structures of the *Penicillium amagasakiense* and *Aspergillus niger* glucose oxidases as a basis for modeling substrate complexes. *Acta Crystallogr. D55*, 969–977.
32. Wohlfahrt, G., Trivic, S., Zeremski, J., Pericin, D., and Leskovac, V. (2004) The chemical mechanism of action of glucose oxidase from *Aspergillus niger*. *Mol. Cell. Biochem. 260*, 69–83.
33. Rotsaert, F. A., Renganathan, V., and Gold, M. H. (2003) Role of the flavin domain residues, His689 and Asn732, in the catalytic mechanism of cellobiose dehydrogenase from *Phanerochaete chrysosporium*. *Biochemistry 42*, 4049–4056.
34. Witt, S., Wohlfahrt, G., Schomburg, D., Hecht, H. J., and Kalisz, H. M. (2000) Conserved arginine-516 of *Penicillium amagasakiense* glucose oxidase is essential for the efficient binding of beta-D-glucose. *Biochem. J. 347*, 553–559.
35. Yin, Y., Sampson, N. S., Vrielink, A., and Lario, P. I. (2001) The presence of a hydrogen bond between asparagine 485 and the pi system of FAD modulates the redox potential in the reaction catalyzed by cholesterol oxidase. *Biochemistry 40*, 13779–13787.
36. Ferreira, P., Ruiz-Duenas, F. J., Martinez, M. J., van Berkel, W. J., and Martinez, A. T. (2006) Site-directed mutagenesis of selected residues at the active site of aryl-alcohol oxidase, an H_2O_2-producing ligninolytic enzyme. *FEBS J. 273*, 4878–4888.
37. Jaenicke, L., and Preun, J. (1984) Chemical modification of hydroxynitrile lyase by selective reaction of an essential cysteine-SH group with alpha, beta-unsaturated propiophenones as pseudo-substrates. *Eur. J. Biochem. 138*, 319–325.
38. Becker, W., and Pfeil, E. (1966) Über das flavinenzym D-oxynitrilase. *Biochem. Z. 346*, 301–321.

39. Zuegg, J., Gruber, K., Gugganig, M., Wagner, U. G., and Kratky, C. (1999) Three-dimensional structures of enzyme-substrate complexes of the hydroxynitrile lyase from *Hevea brasiliensis*. *Protein Sci. 8*, 1990–2000.
40. Gruber, K. (2001) Elucidation of the mode of substrate binding to hydroxynitrile lyase from *Hevea brasiliensis*. *Proteins 44*, 26–31.
41. Hasslacher, M., Schall, M., Hayn, M., Griengl, H., Kohlwein, S. D., and Schwab, H. (1996) Molecular cloning of the full-length cDNA of *(S)* -hydroxynitrile lyase from *Hevea brasiliensis*. Functional expression in *Escherichia coli* and *Saccharomyces cerevisiae* and identification of an active site residue. *J. Biol. Chem. 271*, 5884–5891.
42. Gruber, K., Gartler, G., Krammer, B., Schwab, H., and Kratky, C. (2004) Reaction mechanism of hydroxynitrile lyases of the alpha/beta-hydrolase superfamily: the three-dimensional structure of the transient enzyme-substrate complex certifies the crucial role of LYS236. *J. Biol. Chem. 279*, 20501–20510.
43. Lauble, H., Miehlich, B., Forster, S., Wajant, H., and Effenberger, F. (2001) Mechanistic aspects of cyanogenesis from active-site mutant Ser80Ala of hydroxynitrile lyase from *Manihot esculenta* in complex with acetone cyanohydrin. *Protein Sci. 10*, 1015–1022.
44. Trummler, K., and Wajant, H. (1997) Molecular cloning of acetone cyanohydrin lyase from flax (*Linum usitatissimum*). Definition of a novel class of hydroxynitrile lyases. *J. Biol. Chem. 272*, 4770–4774.
45. Fraaije, M. W., and Mattevi, A. (2000) Flavoenzymes: diverse catalysts with recurrent features. *Trends Biochem. Sci. 25*, 126–132.
46. Lario, P. I., Sampson, N., and Vrielink, A. (2003) Sub-atomic resolution crystal structure of cholesterol oxidase: what atomic resolution crystallography reveals about enzyme mechanism and the role of the FAD cofactor in redox activity. *J. Mol. Biol. 326*, 1635–1650.
47. Fan, F., and Gadda, G. (2005) On the catalytic mechanism of choline oxidase. *J. Am. Chem. Soc. 127*, 2067–2074.
48. Massey, V., Müller, F., Feldberg, R., Schuman, M., Sullivan, P. A., Howell, L. G., Mayhew, S. G., Matthews, R. G., and Foust, G. P. (1969) The reactivity of flavoproteins with sulfite. Possible relevance to the problem of oxygen reactivity. *J. Biol. Chem. 244*, 3999–4006.
49. Massey, V., and Palmer, G. (1966) On the existence of spectrally distinct classes of flavoprotein semiquinones. A new method for the quantitative production of flavoprotein semiquinones. *Biochemistry 5*, 3181–3189.
50. Yemm, R. S., and Poulton, J. E. (1986) Isolation and characterization of multiple forms of mandelonitrile lyase from mature black cherry (*Prunus serotina Ehrh.*) seeds. *Arch. Biochem. Biophys. 247*, 440–445.

BI802162S